

# The Role of Adsorption Species in the Formation of Ag Nanostructures by a Microwave-Polyol Route

Masaharu Tsuji,<sup>\*1,2,3</sup> Kisei Matsumoto,<sup>2,3</sup> Peng Jiang,<sup>1,4</sup> Ryoichi Matsuo,<sup>2,3</sup>  
Sachie Hikino,<sup>1</sup> Xin-Ling Tang,<sup>2</sup> and Khairul Sozana Nor Kamarudin<sup>1,5</sup>

<sup>1</sup>Institute for Materials Chemistry and Engineering, Kyushu University, Kasuga 816-8580

<sup>2</sup>Department of Applied Sciences for Electronics and Materials, Graduate School of Engineering Sciences, Kyushu University, Kasuga 816-8580

<sup>3</sup>CREST, Japanese Science and Technology, Nihonbashi, Tokyo 103-0027

<sup>4</sup>National Center for Nanoscience and Technology, Beijing 100080, P. R. China

<sup>5</sup>Department of Gas Engineering, Faculty of Chemical and Natural Resources Engineering, Universiti Teknologi Malaysia, 81310 UTM Skudai, Johor, Malaysia

Received October 29, 2007; E-mail: tsuji@cm.kyushu-u.ac.jp

The role of adsorption species in reaction solutions has been studied in microwave-polyol synthesis of silver (Ag) nanostructures. When  $\text{Ag}^+$  ions from  $\text{AgNO}_3$  were reduced in ethylene glycol by the addition of  $\text{H}_2[\text{PtCl}_6]$  and poly(vinylpyrrolidone) (PVP), a mixture of one-dimensional (1-D) nanorods and nanowires and 3-D spherical, cubic, and triangular-bipyramidal nanoparticles was obtained within three minutes. It has been previously believed that PVP acts as a surfactant and its selective adsorption on {100} facets results in pentagonal 1-D nanorods or nanowires and cubic and triangular-bipyramidal nanocrystals. We found here that these Ag products could also be formed without the addition of PVP in the presence of  $\text{Cl}^-$  ions, though their yields were lower than those in the presence of PVP by a factor of  $\approx 300$ . These results indicate that  $\text{Cl}^-$  anions can also act as adsorption species to assist the formation of these Ag nanostructures. It is concluded that the difference in the adsorption ability of different species in solution on Ag nanostructures determines final shapes, sizes, and yields of formed Ag nanostructures.

Recently, control of metallic nanostructures has been the focus of intensive research because of their shape-dependent chemical and physical properties.<sup>1</sup> Among them, nanostructured Au and Ag have attracted considerable attention mainly as a result of their remarkable optical properties and numerous applications in the fields such as catalysts, surface plasmonics, surface-enhanced Raman scattering, and chemical and biological sensing.<sup>1–3</sup> Different chemical and physical properties of metallic crystals arise from different crystal surface orientation. For example, the {111}, {100}, and {110} surfaces of a face-centered cubic (fcc) metal such as gold and silver have very different surface atom densities, electronic structures, and chemical reactivities.<sup>4</sup> Therefore, the controllable preparation of nanocrystals with different shapes and exposed surfaces is very important and challenging.

The polyol method is a typical technique for the preparation of metallic nanocrystals in solutions by reducing their ionic salts. In general, a mixture of reaction reagents and a polymer surfactant such as poly(vinylpyrrolidone) (PVP) in ethylene glycol (EG) is heated in an oil bath for several hours.<sup>5</sup> As an alternative, microwave (MW) can be used as a heating source to initiate and rapidly prepare metallic nanoparticles in the polyol system. This method, called MW-polyol, has been applied to rapid syntheses of anisotropic Ag nanostructures such as rods and wires, cubes, truncated-polyhedrons, and bipyramids within a few minutes.<sup>6–9</sup>

It was previously believed that the key to the formation of such one-dimensional (1-D) Ag nanocrystals as rods and wires by using the polyol method is the use of seeding material such as Pt and PVP as a protecting reagent.<sup>6,7,10</sup> We have recently studied the role of Pt catalysts by using  $\text{H}_2[\text{PtCl}_6] \cdot 6\text{H}_2\text{O}$  and bisacetylacetonatoplatinum(II)  $[\text{Pt}(\text{acac})_2]$ , and found that the key factor in Pt reagents for the preparation of such Ag nanocrystals as cubes, bipyramids, and 1-D materials with well-defined facets is not Pt catalytic seeds but  $\text{Cl}^-$  anions produced from decomposition of  $\text{H}_2[\text{PtCl}_6]$ .<sup>8</sup> This suggestion was confirmed from another different experiment in the absence of Pt seeds by the addition of NaCl or KCl as a  $\text{Cl}^-$  source to  $\text{AgNO}_3/\text{PVP}/\text{EG}$  solutions. We concluded that oxidative etching of unstable spherical particles by  $\text{Cl}^-/\text{O}_2$  (dissolved in EG) led to anisotropic nanocrystals in high yields. We have also studied the effects of concentration and molecular weight of PVP for the formation of Ag nanostructures using three different chain-lengths of PVPs ( $M_w = 10, 40, \text{ and } 360 \text{ k}$ ).<sup>7b–7d</sup> It has been found that the shapes of obtained Ag nanostructures depend strongly on the concentration and chain length of PVP. There is an appropriate concentration of PVP for the preparation of 1-D products in high yields, whereas PVPs with longer chain length are favorable for the preparation of long 1-D products in high yields. The generally accepted viewpoint for the preparation of cubic, bipyramidal, and 1-D Ag nanocrystals having predominantly {100} facets in fcc crystals is

the selective adsorption of PVP to these facets, which reduces the relative growth rate along the crystalline plane direction.

The preparation of Ag nanowires by using a MW-polyol method has recently been studied by Gou et al.<sup>9</sup> They used a  $\text{AgNO}_3/\text{NaCl}/\text{PVP}/\text{EG}$  system and discussed roles of oxidative etching by  $\text{Cl}^-/\text{O}_2$  (dissolved in EG) and irradiation effects of MW. They reported that the ends of the nanowires are evolving sites with sharp defects. Therefore, these positions may reach higher temperatures than the wire midsection and accumulate charge due to polarization by the microwave field. The elevated temperature and charge localization may further designate the wire ends as preferential sites for deposition of  $\text{Ag}^0$ , with PVP already selectively protecting the longitudinal axis of the nanowire. They predicted that the selective protection of side facets by PVP assists the 1-D growth of Ag nanowires under MW irradiation. However, no definite experimental evidence for this explanation has been obtained.

Although polymer surfactants like PVP have been widely used for the preparation of anisotropic Ag nanostructures, few studies have been carried out on their real role except for pioneering works by Caswell et al.<sup>11</sup> and Zhang et al.<sup>12</sup> Caswell et al. reported a method to make crystalline Ag nanowires in water, in the absence of a surfactant or polymer to direct nanoparticle growth and without externally added seed crystallites. The reaction was one in which silver salt was reduced to metallic Ag at  $100^\circ\text{C}$  by sodium citrate in the presence of NaOH. They thought that the citrate played multiple roles in the crystal growth of 1-D Ag materials. It not only strongly coordinates  $\text{Ag}^+$  ions to form complexes but also is responsible for the reduction of  $\text{Ag}^+$  ions to metallic Ag as well as acts as a capping agent. Zhang et al.<sup>12</sup> synthesized Ag nanowires by simply reducing  $\text{Ag}^+$  ions with reductants such as glucose, sodium citrate, and sodium hypophosphite, in the absence of surfactants at temperatures ranging from  $80$  to  $200^\circ\text{C}$ . Regardless of the reductants, the Ag nanowires prepared at a given temperature were uniform in diameters ranging from  $30$  to  $50\text{ nm}$ . There is a high possibility that these reductants involving citrate act as capping agents, as that in the case of Caswell et al.<sup>11</sup>

In the present study, we investigated the role of adsorption species including PVP in reaction solution for the crystal growth of Ag nanostructures. It was found that 1-D Ag nanostructures, cubes, and bipyramids with well-defined facets could be prepared even without the addition of surfactant in the presence of a small amount of  $\text{Cl}^-$  anions, though their yields are very low in comparison with those in the presence of PVP. Since PVP is widely used as a surfactant for the preparation of many metallic nanoparticles using polyol methods, the present results provide a new fundamental insight into the role of various adsorption species in the formation of Ag nanostructures by a MW route.

### Experimental

The MW-polyol apparatus used in this study was similar to that reported previously.<sup>6–8</sup> A MW oven was modified by installing a condenser and thermocouple through ceiling holes and a Teflon-coated magnetic stirrer at the bottom. A three-necked flask ( $100\text{ mL}$ ) was placed in the MW oven and connected to the condenser. A solution containing only  $\text{AgNO}_3$  or a mixture

of  $\text{AgNO}_3/\text{H}_2[\text{PtCl}_6]\cdot 6\text{H}_2\text{O}$ ,  $\text{AgNO}_3/\text{H}_2[\text{PtCl}_6]\cdot 6\text{H}_2\text{O}/\text{PVP}$ , or  $\text{AgNO}_3/\text{NaCl}$  in EG was irradiated with MW (Shikoku Keisoku:  $\mu$  Reactor) in a continuous wave (CW) mode at  $400$  or  $650\text{ W}$  (typically  $650\text{ W}$ ). Reagent concentrations in each experiment are shown in figure captions. The solution was rapidly heated to the boiling point of EG ( $198^\circ\text{C}$ ) after about  $1.5\text{ min}$  and held at this temperature for  $1.5\text{ min}$ . Thus, the total heating time was  $3\text{ min}$ . After MW irradiation, transmission electron microscope (TEM) images of products in the supernatant and the precipitate were measured in the  $\text{AgNO}_3/\text{H}_2[\text{PtCl}_6]\cdot 6\text{H}_2\text{O}$  and  $\text{AgNO}_3/\text{NaCl}$  systems. The supernatant was centrifuged at  $13000\text{ rpm}$  for  $60\text{ min}$  after removing precipitate, when products in the supernatant were obtained. On the other hand, no precipitate was obtained from the  $\text{AgNO}_3/\text{H}_2[\text{PtCl}_6]\cdot 6\text{H}_2\text{O}/\text{PVP}$  system. In this case, all product solutions were centrifuged at  $13000\text{ rpm}$  for  $60\text{ min}$ . The precipitate obtained after centrifugal separation was collected, and then redispersed in deionized water for the TEM observation. Specimens containing Ag nanostructures were prepared by dropping the colloidal solutions of supernatant or precipitate on Cu grids covered with carbon. Absorption spectra of the product solutions were measured in the UV–visible(vis)–near infra (NIR) region using a Shimadzu UV-3600 spectrometer.

### Results and Discussion

**Effects of PVP.** To examine the effects of PVP, the  $\text{AgNO}_3$  ( $46.5\text{ mM}$ )/ $\text{H}_2[\text{PtCl}_6]\cdot 6\text{H}_2\text{O}$  ( $115\text{ }\mu\text{M}$ )/PVP ( $264\text{ mM}$ )/EG solution was irradiated with MW for  $3\text{ min}$  in the presence or absence of PVP. In the presence of PVP no precipitate was obtained. A typical TEM image of products in the supernatant is shown in Fig. 1a, where a mixture of 1-D nanorods or nanowires with an average length of  $\approx 1\text{ }\mu\text{m}$ , spherical nanoparticles with an average diameter of  $\approx 60\text{ nm}$ , and a small amount of cubic and bipyramid crystals were observed. This finding is consistent with our previous study using PVP ( $M_w = 360\text{ k}$ ).<sup>7d</sup> On the other hand, a significant amount of precipitate was obtained in the absence of PVP under the same reaction conditions. In order to know whether some extra products still existed in the supernatant, TEM images of the products in the supernatant were measured after centrifugal separation. Figures 1b–1e show typical TEM images of the products. A small amount of 1-D nanorods and nanowires (Figs. 1b-1 and 1b-2: yield 21%), cubic crystal (Fig. 1c-1: 6%), triangular-bipyramidal particles (Fig. 1c-2: 4%), flower-type product (Fig. 1d: 0.5%), and sheet (Fig. 1e: 0.5%) can be observed in the TEM images besides spherical particles as major products (68%). Selected area electron diffraction patterns measured for cubes and bipyramids gave square spots, indicating that these crystals are surrounded by  $\{100\}$  facets of fcc Ag crystals (Figs. 1c-1 and 1c-2). Lengths of some Ag nanowires even reached more than  $10\text{ }\mu\text{m}$ , which is longer than those prepared in the presence of PVP ( $\approx 1\text{ }\mu\text{m}$ ) under our MW heating experiments. The sizes of observed Ag cubes and bipyramids ( $200$ – $400\text{ nm}$ ) are also larger than those obtained in the presence of PVP ( $40$ – $70\text{ nm}$ ). When the precipitates were viewed by TEM, various kinds of products such as large spherical particles, 1-D wires, and decahedral particles were found (see Figs. 2a–2d). These results indicate that larger or longer anisotropic Ag nanostructures can be produced even in the absence of PVP, though their amounts were smaller than those in its presence.

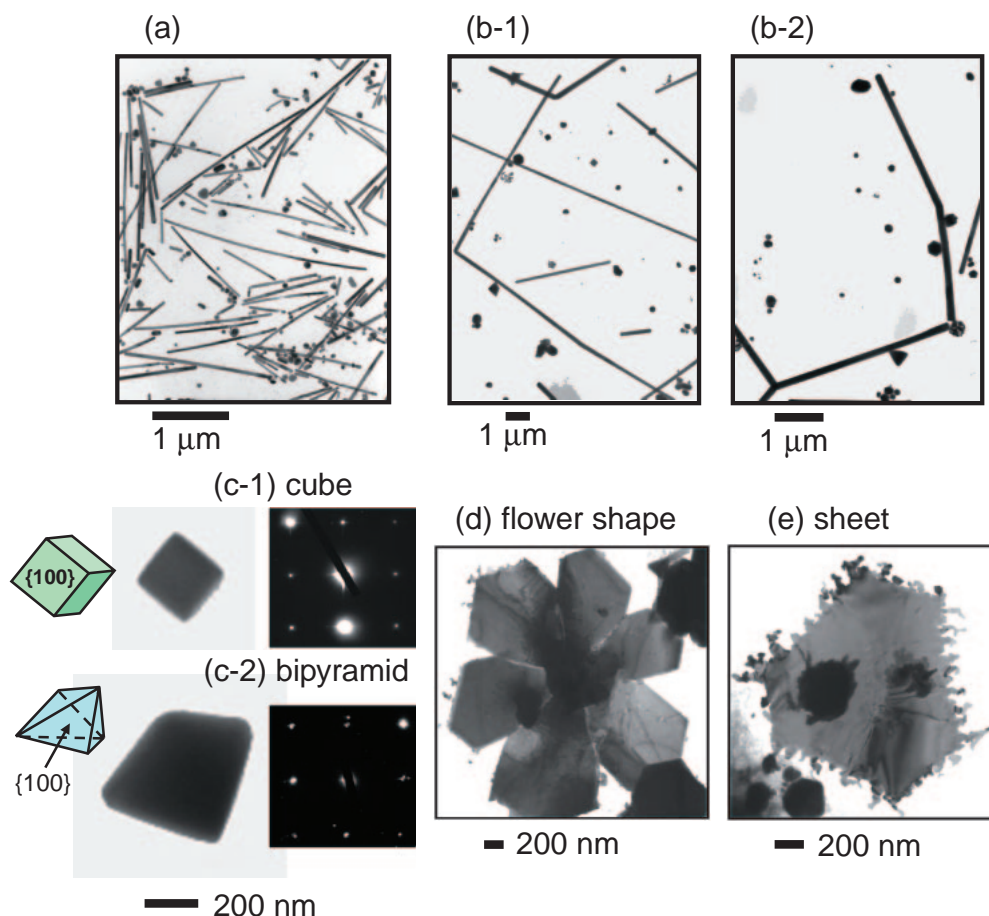


Fig. 1. TEM images of Ag nanostructures of surfactants prepared from (a)  $\text{AgNO}_3$  (46.5 mM)/ $\text{H}_2[\text{PtCl}_6] \cdot 6\text{H}_2\text{O}$  (115  $\mu\text{M}$ )/PVP (264 mM)/EG and (b)–(e)  $\text{AgNO}_3$  (46.5 mM)/ $\text{H}_2[\text{PtCl}_6] \cdot 6\text{H}_2\text{O}$  (115  $\mu\text{M}$ )/EG solutions. Selected area electron diffraction patterns of cube and bipyramid are shown in (c-1) and (c-2). The MW power and heating time was 650 W and 3 min, respectively.

In order to estimate the relative amounts of Ag nanostructures in the supernatant in the absence and presence of PVP, absorption spectra were measured in the UV–vis–NIR region. It has been well known that absorption spectra of Ag nanostructures depend strongly on the shapes and sizes of the nanostructures.<sup>7,8,10,13–15</sup> The surface plasmon resonance (SPR) band of spherical silver nanoparticles with diameters of 20–40 nm has a peak at  $\approx 410$  nm. Its peak shifts to  $\approx 480$  nm with increasing diameter from 40 to 90 nm. The dominant peaks of SPR bands of rods and wires appear at  $\approx 350$  and  $\approx 380$  nm. According to a recent report by Gao et al.,<sup>15c,15d</sup> these two peaks were attributed to the transversal modes of the 1-D products with pentagonal cross sections, corresponding to the out-of-plane quadrupole resonance and out-of-plane dipole resonance modes, respectively. When the  $\approx 410$  nm peak due to spherical particles is strong, it overlaps with the  $\approx 380$  nm peak. In such a case, the  $\approx 380$  nm peak of the 1-D products is not clearly observed. When long Ag nanowires are produced, a long tail band is observed above 450 nm. Gao et al.<sup>15d</sup> attributed this tail band to the overlapping of the in-plane quadrupole and dipole resonance modes of nanowires with peaks at 445 and 514 nm, respectively. SPR bands of cubic crystals (edge length:  $\approx 80$  nm), triangular-bipyramidal crystals (edge length: 75 nm), and five twin decahedrons (edge length:  $\approx 80$  nm) of Ag have been observed at 320–800 nm with a peak at

$\approx 470$  nm, 320–900 nm with a peak at  $\approx 520$  nm, and 320–900 nm with a peak at 569 nm, respectively.<sup>14,15</sup> When cubic, triangular, and decahedral Ag particles are produced, the above peaks also overlap with the SPR bands of spherical and 1-D particles.

Figure 3 shows a typical absorption spectrum of the supernatant in the absence of PVP. For comparison, that obtained in the presence of PVP (264 mM) is also shown. In both cases, SPR bands due to isotropic and anisotropic Ag nanostructures with a peak at  $\approx 420$  or  $\approx 450$  nm are observed in the 320–1300 nm region. In the presence of PVP, the SPR band has a peak at  $\approx 420$  nm and the tail band above 600 nm is strong, indicating that SPR bands of spherical and 1-D particles overlap. On the other hand, a peak shift to about  $\approx 450$  nm and a broad tail band are observed in the absence of PVP. This implies that the contribution of spherical particles is small and long 1-D particles are produced even in the absence of PVP. These observations are consistent with the TEM images shown in Figs. 1a and 1b. The absorbance of SPR peak in the 420–450 nm region in the absence of PVP was weaker than that in the presence of PVP by factors of  $\approx 300$  taking account of a dilution factor of solution. This shows that the total yield of Ag nanoparticles in supernatant obtained in the absence of PVP was lower than that in the presence of PVP by more than two orders of magnitude.

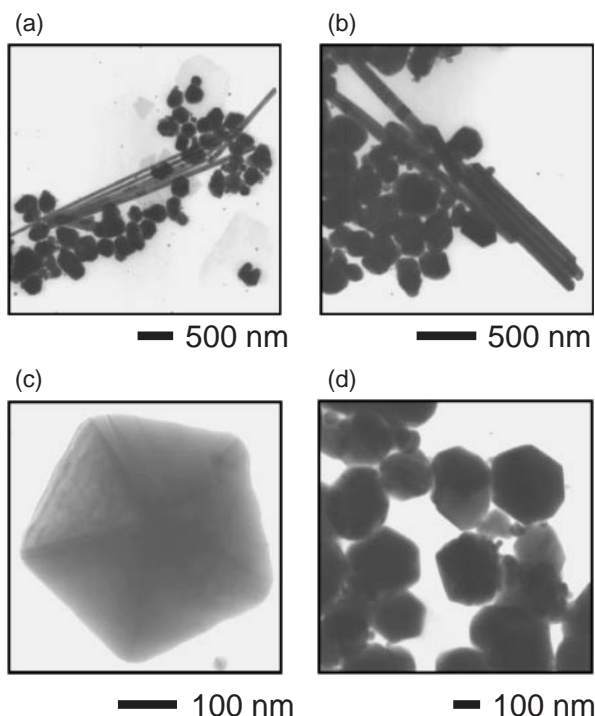


Fig. 2. TEM images of Ag nanostructures of precipitates prepared from  $\text{AgNO}_3$  (46.5 mM)/ $\text{H}_2[\text{PtCl}_6] \cdot 6\text{H}_2\text{O}$  (115  $\mu\text{M}$ )/EG solutions. Other conditions were the same as those in Fig. 1.

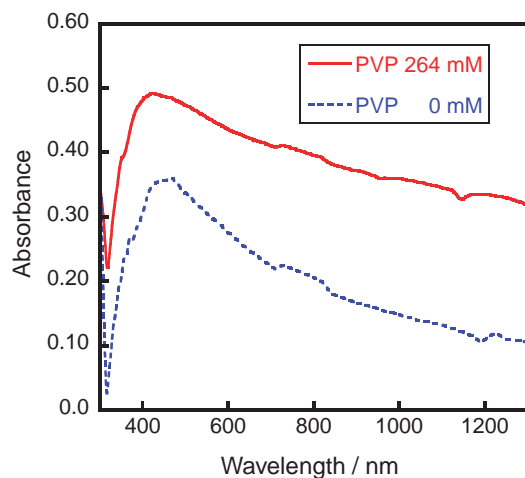


Fig. 3. UV-vis-NIR absorption spectra obtained from  $\text{AgNO}_3$  (46.5 mM)/ $\text{H}_2[\text{PtCl}_6] \cdot 6\text{H}_2\text{O}$  (115  $\mu\text{M}$ )/PVP (264 mM)/EG and  $\text{AgNO}_3$  (46.5 mM)/ $\text{H}_2[\text{PtCl}_6] \cdot 6\text{H}_2\text{O}$  (115  $\mu\text{M}$ )/EG solutions. The former solution was diluted by a factor of 200 before spectral measurement.

**Effects of MW Power.** Figures 4a–4c show TEM images of Ag products in the supernatant obtained in the absence of PVP at a low MW power of 400 W. It should be noted that product shapes are different from those at 650 W (Figs. 1b–1e). At 400 W, bundle-like 1-D Ag products (Figs. 4a and 4b) and flexible string-like 1-D Ag products (Figs. 4b and 4c) are obtained. Figure 4d shows a TEM image of the products in the precipitates, where a mixture of 1-D products and large spherical particles are observed. Similar bundle-like

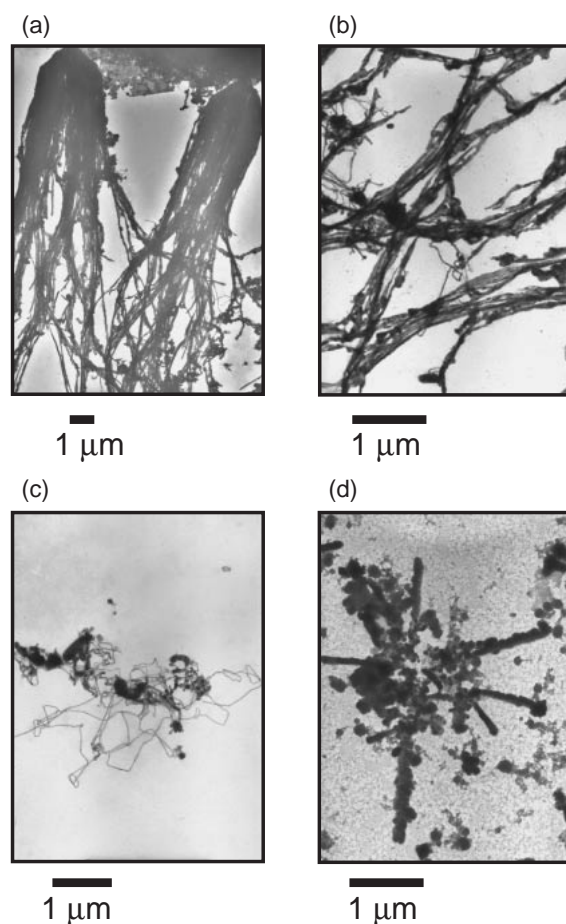


Fig. 4. TEM images of Ag nanostructures of (a–c) surfactants and (d) precipitates prepared from  $\text{AgNO}_3$  (46.5 mM)/ $\text{H}_2[\text{PtCl}_6] \cdot 6\text{H}_2\text{O}$  (115  $\mu\text{M}$ )/EG solution. The MW power and heating time was 400 W and 3 min, respectively.

1-D Ag products have been obtained by Caswell et al.<sup>11</sup> without addition of surfactant. Flexible string-like 1-D Ag products have also been obtained by Sun et al.<sup>10d</sup> in the polyol synthesis of Ag nanowires under oil-bath heating. In the present MW-polyol synthesis of Ag nanostructures, non-straight bundle-like and string-like 1-D Ag products are formed in the absence of PVP at 400 W. This indicates that more lattice defects or twinning structures are probably produced in the 1-D Ag nanostructures in the absence of PVP at a low MW power, so that flexible structures of 1-D products may be synthesized. The formation of cubes and bipyramids having {100} facets were not observed at 400 W. On the basis of the above results, a high MW power of 650 W is necessary for the syntheses of highly crystalline 1-D products, cubes, and bipyramids with well-defined facets having few lattice defects. It is known that Ag nanoparticles are heated under MW irradiation due to MW field-induced electron polarization and charge localization.<sup>9</sup> Since such MW irradiation effects become strong at high power, highly crystalline Ag nanocrystals are produced at 650 W.

**Effects of  $\text{Cl}^-$  in the Absence of PVP.** We have recently found that  $\text{Cl}^-$  anions resulting from decomposition of  $\text{H}_2[\text{PtCl}_6]$  in EG play a significant role for the formation of Ag nanostructures with well-defined facets.<sup>8</sup> However, all of



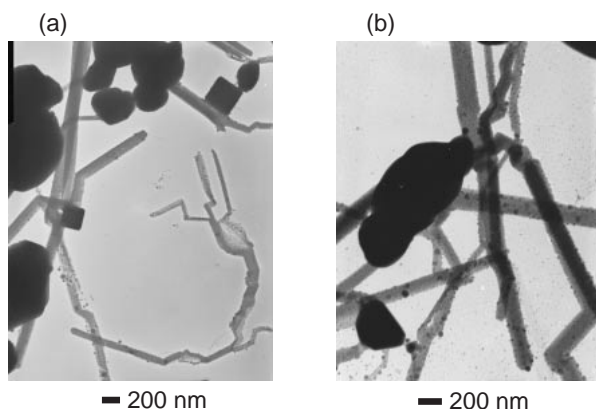


Fig. 5. TEM images of Ag nanostructures of surfactants prepared from  $\text{AgNO}_3$  (46.5 mM)/ $\text{NaCl}$  (690  $\mu\text{M}$ )/EG solution. Other conditions were the same as those in Fig. 1.

our previous experiments were carried out in the presence of PVP. Therefore, no information on the effects of  $\text{Cl}^-$  anions in the absence of PVP was obtained. The  $\text{Cl}^-$  concentration of  $\text{H}_2[\text{PtCl}_6] \cdot 6\text{H}_2\text{O}$  (115  $\mu\text{M}$ )/EG solution after MW irradiation for 3 min was measured by using a titration apparatus (Kyoto Electronic AT610). A standard  $\text{AgNO}_3$  solution was used as a titration reagent. The  $\text{Cl}^-$  concentration was estimated to be 670  $\mu\text{M}$ . This implies that  $\text{Cl}$  in  $\text{H}_2[\text{PtCl}_6]$  is nearly completely converted to  $\text{Cl}^-$  under our experimental conditions.  $\text{Cl}^-$  anions can selectively etch spherical particles, whereas cubes, triangular bipyramids, and pentagonal 1-D rods and wires can survive oxidative etching by  $\text{Cl}^-/\text{O}_2$  (dissolved in EG) and evolve into larger crystals in the presence of PVP under MW heating.<sup>8</sup> When Ag nanoparticles were prepared without the addition of  $\text{H}_2[\text{PtCl}_6] \cdot 6\text{H}_2\text{O}$  and PVP in the present study, dominant products were aggregates of Ag particles and only a very small amount of spherical Ag particles existed in the surfactant. In order to examine effects of Pt catalysts and  $\text{Cl}^-$  anions in the absence of PVP, Ag nanoparticles were synthesized from  $\text{AgNO}_3/\text{NaCl}/\text{EG}$  solution. In this case,  $\text{NaCl}$  was added as a  $\text{Cl}^-$  anion source. For convenient comparison to the case of  $\text{H}_2[\text{PtCl}_6] \cdot 6\text{H}_2\text{O}$ , 690  $\mu\text{M}$  of  $\text{NaCl}$  was added into the  $\text{AgNO}_3/\text{EG}$  solution. Figures 5a and 5b show TEM images obtained from  $\text{AgNO}_3/\text{NaCl}/\text{EG}$  solution, where long branched 1-D products and large cubes (200–300 nm) were observed besides large spherical particles. A number of small spherical particles are attached to 1-D products in some cases because no surfactant was added. This finding implies that a key reagent for the preparation of Ag products with well-defined facets is  $\text{Cl}^-$  anion resulting from  $\text{H}_2[\text{PtCl}_6] \cdot 6\text{H}_2\text{O}$  and  $\text{NaCl}$  under MW heating even in the absence of PVP.

**Growth Mechanisms of Silver Nanostructures.** The polyol method has been widely applied to the preparation of such anisotropic Ag nanostructures as nanowires and cubes in high yields.<sup>10,14,15</sup> In general, EG solutions were initially heated to about 160  $^\circ\text{C}$  in an oil bath for about one hour to remove a small amount of impurities such as  $\text{H}_2\text{O}$ . Then,  $\text{AgNO}_3$  and PVP were injected drop-wise via syringe pumps. Ag nanowires were prepared by using Pt or Ag seeds. They could also be obtained without using seeds. In such cases, Ag seeds formed at the very beginning of the drop-wise addition could serve as the

seeds for the following growth process. When the addition rates of reagents were fast, only spherical nanoparticles were obtained. Thus, growth of anisotropic nanostructures like nanowires usually requires slow reaction conditions to reduce the number of nucleation sites formed or equilibrium dissolution of these nucleation sites to promote site-specific growth. In the MW-polyol method, we use simple one-pot syntheses without using seeded growth or drop-wise addition, and reactions are completed after only 3 min. Such a rapid synthesis of Ag nanowires is difficult without using MW heating. Under MW heating, we<sup>6–8</sup> and Gou et al.<sup>9</sup> found that  $\text{Cl}^-/\text{O}_2$  (dissolved in EG) and PVP are key reagents for the formation of nanowires, cubes, and bipyramids. The effects of  $\text{Cl}^-$  were attributed to shape selective oxidative etching and a decrease in the concentration of free  $\text{Ag}^+$  ions by the formation of  $\text{AgCl}$  leading to slow reaction conditions. Although effects of  $\text{Cl}^-$  were discussed in detail, real roles of PVP under MW irradiation have not been known.

In the present study, the effects of PVP in the preparation of Ag nanostructures under MW irradiation were examined. Wet chemical syntheses have been successfully applied to the preparation of various Ag nanostructures. On the basis of our recent findings for the preparation of Ag nanostructures<sup>7</sup> and Au@Ag core-shell nanoparticles,<sup>16</sup> the growth mechanism of each Ag nanostructure in MW-polyol processes is shown in Fig. 6. It is suspected that spherical particles, cubes, triangular-bipyramids, and 1-D rods and wires grow from small spherical, cuboctahedral, single-twin triangular-plate like, and decahedral particles, respectively. It has been believed that a capping agent like PVP is necessary for the preparation of highly crystalline cubes, bipyramids, and 1-D rods and wires. For example, for the preparation of Ag nanowires, a capping reagent such as PVP has been employed to direct the 1-D growth.<sup>6–10</sup> The proposed mechanism is that the Ag nanowires are formed by initiation of multiply twinned decahedral Ag seed nanoparticles (process (4) in Fig. 6) and subsequent anisotropic growth along the  $[110]$  direction. In the process,  $\{100\}$  facets of the 1-D Ag nanowires are tightly covered by PVP molecules, while each tip surrounded by five  $\{111\}$  facets at two ends of the Ag nanowires is loosely covered by PVP (case (a) in process (4): Fig. 6). Therefore, two highly reactive ends result in rapid reduction of deposition of Ag atoms on them and finally form an elongated decahedron, i.e., five-twinned 1-D Ag nanowire. We have confirmed the validity of this explanation by the preparation of Au@Ag core-shell rods using Au decahedral particles.<sup>16</sup> As  $\{100\}$  surfaces are more active than  $\{111\}$  surfaces, it is obvious that passivation of  $\{100\}$  facets by surfactants such as PVP is necessary for 1-D evolution. This mechanism is conceivable for the growth of 1-D Ag products in the presence of surfactants.

However, in the present case, our experimental results, especially the occurrence of Ag products with well-defined  $\{100\}$  facets such as cubes, can not be well understood by the above mechanism involving surfactants because no surfactant exists in our MW (650 W) reaction systems. In general, from the view point of thermodynamics, Ag  $\{100\}$  facets have a slightly higher surface energy than  $\{111\}$  facets.<sup>17</sup> The occurrence of the Ag nanostructures with  $\{100\}$  facets means that the higher energy facets must be stabilized by special

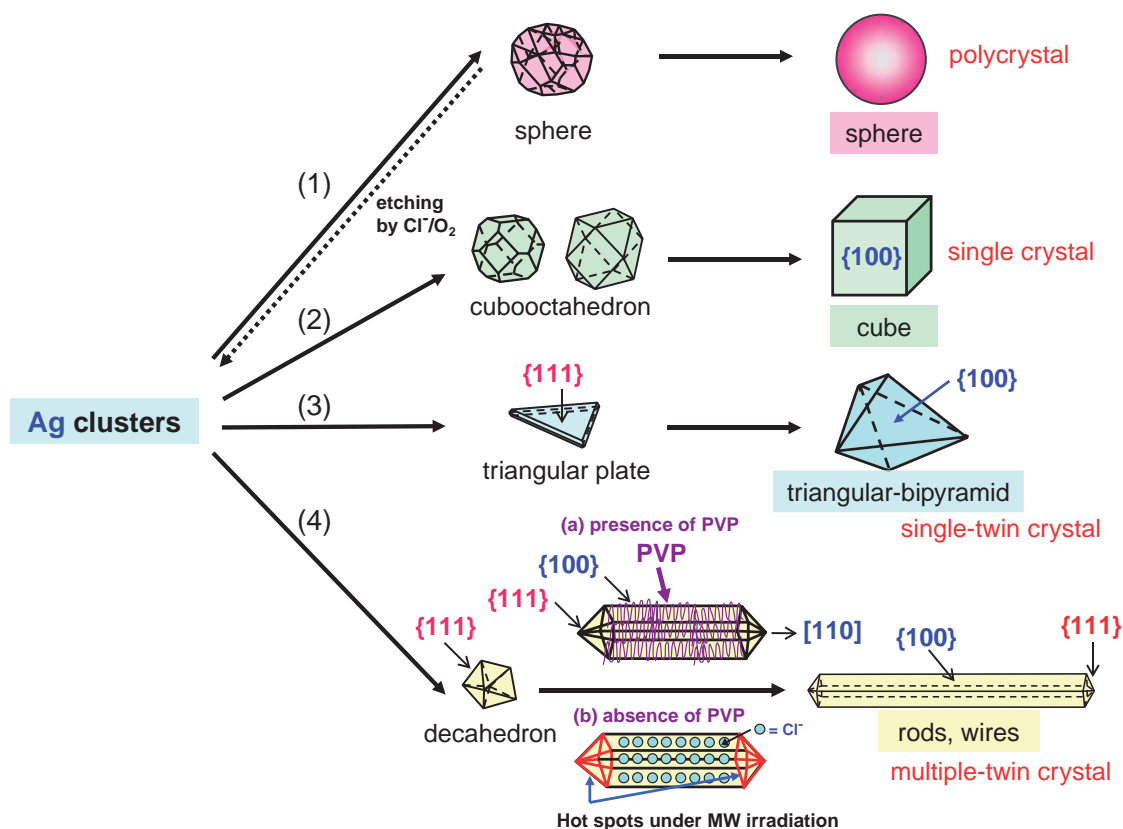


Fig. 6. Growth mechanism of Ag nanostructures under MW heating.

adsorption of certain species to greatly decrease the surface energy of the system. In our case,  $\text{Cl}^-$  ions and other species in solutions could possibly act as the adsorption species. Therefore, the presence of them can stabilize  $\{100\}$  facets to favor the formation of cubic or other Ag nanostructures with  $\{100\}$  facets. It is worth noting that small spherical Ag nanoparticles are produced in the presence of PVP and  $\text{Cl}^-$ , whereas larger spherical particles grow in the absence of PVP even in the presence of the same amount of  $\text{Cl}^-$ . This is probably due to the fact that the growth rate of spherical particles without surfactant is faster than their etching rate by  $\text{Cl}^-$  ions/ $\text{O}_2$  (dissolved in EG), so that large spherical particles grow in high yields. On the other hand, the etching rate of small seeded spherical particles protected by PVP is faster than their growth rates, so they have more opportunities to dissolve in EG (see dotted line in process (1): Fig. 6). Since the protection ability of  $\text{Cl}^-$  and other species is weaker than that of PVP, larger sizes and longer lengths of Ag crystals are produced in the absence of PVP.

Another remarkable feature in the absence of PVP is the formation of a large amount of multiply bent 1-D Ag product at a MW power of 650 W. Similar products have been observed in our two-step synthesis of 1-D Ag products.<sup>7d</sup> These products are probably formed by connection of two  $\{111\}$  facet ends from shorter adjacent 1-D Ag nanorods, as reported previously.<sup>7d</sup> Since the protection of  $\{111\}$  facets by the surfactant is absent, the probability of the formation of multiply bent 1-D Ag products becomes large. Interestingly, bundle-like and flexible string-like 1-D Ag assemblies are found in obtained products, too (see Figs. 4a–4c). Although the formation mechan-

isms of the bundle-like and flexible string-like Ag products are still not clear, the absence of PVP promotes the formation of these products.

Here, we would like to discuss the role of PVP in the preparation of silver nanostructures. The most significant finding in this study is that 1-D products, cubes, and bipyramids, which are major products in the  $\text{AgNO}_3/\text{H}_2[\text{PtCl}_6] \cdot 6\text{H}_2\text{O}/\text{PVP}/\text{EG}$ ,  $\text{AgNO}_3/\text{NaCl}/\text{PVP}/\text{EG}$ , and  $\text{AgNO}_3/\text{KCl}/\text{PVP}/\text{EG}$  solutions<sup>6–9</sup> under MW heating, can be produced even in the absence of PVP. It can be concluded that PVP is not necessary for the formation of highly crystalline Ag 1-D nanowires, cubes, and bipyramids, but interface adsorption by certain species in solution must take place in order to favor emergence of special crystalline facets such as  $\{100\}$ . It is probably the adsorption ability of different species in solution that finally determines the shapes and sizes of formed Ag nanostructures. In this case, PVPs do not contribute to the formation of each seeded structure of anisotropic products. The yields of anisotropic products in the absence of PVP were much lower than those in the presence of PVP. Thus, the role of PVP is protection of aggregation of seeded structures of anisotropic products and enhancement of face-selective growth of anisotropic products by the protection of  $\{100\}$  facets. This means that well-known face-selective protection mechanism by PVP for the anisotropic growth of Ag nanostructures really operates and it is important for their syntheses in high yields without aggregation.

**Irradiation Effects of MW for the Preparation of Anisotropic Ag Nanostructures.** In our study, we used MW heating instead of conventional oil-bath heating. Suzuki et al.<sup>18a</sup>

have recently investigated effects of MW irradiation on metallic nanoparticles by using frequency response analysis and on water and a dilute saline solution by molecular dynamics simulation methods, respectively. They found that metallic nanoparticles are heated by skin effects of MW penetrating inside nanoparticles. Such a local heating of Ag nanowires has been observed by Gou et al. by leaving Ag nanowires under MW fields in air.<sup>9</sup> It is suspected that MW heating promotes nanowire growth by a local “hot spot” effect at the wire ends. These positions may reach even higher temperatures than the wire midsection and accumulate charge due to polarization by the MW field. The elevated temperature and charge localization further designate the wire ends as preferential sites for the deposition of Ag<sup>0</sup>, because PVPs already selectively protect the longitudinal axis of the nanowire. In the study, we found that small amounts of Ag nanowires and other Ag nanocrystals surrounded by {100} facets were formed even in the absence of PVP. This means that 1-D growth of Ag nanowires can occur without protection of side facets by PVP. It is highly likely that a local “hot spot” effect at the wire ends occurs even in the absence of PVP. In such a case, Cl<sup>−</sup> anions and other species probably act as weak protection agents in the AgNO<sub>3</sub>/H<sub>2</sub>[PtCl<sub>6</sub>]·6H<sub>2</sub>O/EG and AgNO<sub>3</sub>/NaCl/EG systems (see case (b) in process (4): Fig. 6).

According to a simulation by Tanaka and Sato,<sup>18b</sup> a diluted NaCl solution is significantly more heated than pure water by MW irradiation. This is due to rapid heating of salt ions, especially large salt ions like Cl<sup>−</sup>, through field-induced motion by the MW electric field and energy transfer by the interactions between salt ions and water molecules. Therefore, we think that the etching rate of spherical Ag particles by Cl<sup>−</sup> anions will be accelerated under MW irradiation due to such an effect, that is, much faster than the case by normal oil-bath heating. This MW irradiation effect will also operate in the preparation of Ag nanostructures in the absence of PVP. These effects will be especially important for the preparation of highly crystalline Ag nanostructures at high MW power.

### Conclusion

Although anisotropic Ag nanostructures can be prepared by MW-polyol methods by using AgNO<sub>3</sub>/H<sub>2</sub>[PtCl<sub>6</sub>]·6H<sub>2</sub>O/PVP/EG and AgNO<sub>3</sub>/NaCl/PVP/EG systems, whether PVP is necessary for the preparation of such nanostructures has not been demonstrated. In the present study, the roles of PVP and other adsorption species have been studied in MW-polyol synthesis of anisotropic silver nanostructures for the first time. It was previously believed that 1-D Ag nanostructures can only be produced in the presence of a capping agent such as PVP due to face selective adsorption of PVP. However, we found here that small amounts of Ag 1-D nanorods or nanowires, and cubic and triangular-bipyramidal nanocrystals could be produced in the supernatant without the addition of PVP in the presence of Cl<sup>−</sup>. These results indicate that PVP is not necessary for the formation of these highly crystalline nanocrystals, but interface adsorption by certain species in solution must take place in order to ensure emergence of special crystalline facets such as {100}. Obviously, Cl<sup>−</sup> ions and other possible species in the reaction solution can fulfill the role of adsorption reagents too. In fact, it is probably the difference

of adsorption ability among various adsorption species to special Ag nanostructure interfaces that determines final shapes and sizes of Ag nanostructure products. Therefore, by coincidence, PVP is probably the most optimized adsorption reagent for the mass production of anisotropic Ag nanostructures surrounded with {100}-type facets.

This work was supported by JST-CREST, Joint Project of Chemical Synthesis Core Research Institutions, and Grant-in-Aid for Scientific Research on Priority Areas “unequilibrium electromagnetic heating” and Grant-in-Aid for Scientific Research (B) from the Ministry of Education, Culture, Sports, Science, and Technology of Japan (Nos. 19033003 and 19310064).

### References

- 1 a) Y. W. Cao, R. C. Jin, C. A. Mirkin, *Science* **2002**, 297, 1536. b) C. Burda, X. B. Chen, R. Narayanan, M. A. El-Sayed, *Chem. Rev.* **2005**, 105, 1025. c) N. L. Rosi, C. A. Mirkin, *Chem. Rev.* **2005**, 105, 1547.
- 2 a) K. Kneipp, Y. Wang, H. Kneipp, L. T. Perelman, I. Itzkan, R. R. Dasari, M. S. Feld, *Phys. Rev. Lett.* **1997**, 78, 1667. b) A. J. Haes, R. P. Van Duyne, *J. Am. Chem. Soc.* **2002**, 124, 10596. c) B. D. Moore, L. Stevenson, A. Watt, S. Flitsch, N. J. Turner, C. Cassidy, D. Graham, *Nat. Biotechnol.* **2004**, 22, 1133.
- 3 a) I. H. El-Sayed, X. H. Huang, M. A. El-Sayed, *Nano Lett.* **2005**, 5, 829. b) X. H. Huang, I. H. El-Sayed, W. Qian, M. A. El-Sayed, *J. Am. Chem. Soc.* **2006**, 128, 2115.
- 4 Z. L. Wang, *J. Phys. Chem. B* **2000**, 104, 1153.
- 5 a) F. Fievet, J. P. Lagier, B. Blin, B. Beaudoin, M. Figlarz, *Solid State Ionics* **1989**, 32–33, 198. b) P.-Y. Silvert, R. Herrera-Urbina, N. Duvauchelle, V. Vijayakrishnan, K. Tekaia-Elhsissen, *J. Mater. Chem.* **1996**, 6, 573. c) P.-Y. Silvert, R. Herrera-Urbina, K. Tekaia-Elhsissen, *J. Mater. Chem.* **1997**, 7, 293. d) M. S. Hegde, D. Larcher, L. Dupont, B. Beaudoin, K. Tekaia-Elhsissen, J. M. Tarascon, *Solid State Ionics* **1996**, 93, 33.
- 6 M. Tsuji, M. Hashimoto, Y. Nishizawa, M. Kubokawa, T. Tsuji, *Chem. Eur. J.* **2005**, 11, 440.
- 7 a) M. Tsuji, Y. Nishizawa, M. Hashimoto, T. Tsuji, *Chem. Lett.* **2004**, 33, 370. b) M. Tsuji, Y. Nishizawa, K. Matsumoto, M. Kubokawa, N. Miyamae, T. Tsuji, *Mater. Lett.* **2006**, 60, 834. c) M. Tsuji, Y. Nishizawa, K. Matsumoto, N. Miyamae, T. Tsuji, X. Zhang, *Colloids Surf., A* **2007**, 293, 185. d) M. Tsuji, K. Matsumoto, N. Miyamae, T. Tsuji, X. Zhang, *Cryst. Growth Des.* **2007**, 7, 311.
- 8 M. Tsuji, K. Matsumoto, P. Jiang, R. Matsuo, X.-L. Tang, K. S. N. Kamarudin, *Colloids Surf., A* **2008**, 316, 266.
- 9 L. Gou, M. Chipara, J. M. Zaleski, *Chem. Mater.* **2007**, 19, 1755.
- 10 a) Y. Sun, B. Gates, B. Mayers, Y. Xia, *Nano Lett.* **2002**, 2, 165. b) Y. Sun, Y. Xia, *Adv. Mater.* **2002**, 14, 833. c) Y. Sun, Y. Yin, B. Mayers, T. Herricks, Y. Xia, *Chem. Mater.* **2002**, 14, 4736. d) Y. Sun, B. Mayers, Y. Xia, *Nano Lett.* **2003**, 3, 675. e) Y. Sun, B. Mayers, T. Herricks, Y. Xia, *Nano Lett.* **2003**, 3, 955. f) J. Chen, B. J. Wiley, Y. Xia, *Langmuir* **2007**, 23, 4120.
- 11 K. K. Caswell, C. M. Bender, C. J. Murphy, *Nano Lett.* **2003**, 3, 667.
- 12 S.-H. Zhang, Z.-Y. Jiang, Z.-X. Xie, X. Xu, R.-B. Huang, L.-S. Zheng, *J. Phys. Chem. B* **2005**, 109, 9416.

- 13 A. Henglein, *J. Phys. Chem.* **1993**, *94*, 5457.
- 14 a) B. Wiley, Y. Sun, B. Mayers, Y. Xia, *Chem. Eur. J.* **2005**, *11*, 454. b) B. J. Wiley, S. H. Im, Z.-Y. Li, J. McLellan, A. Siekkinen, Y. Xia, *J. Phys. Chem. B* **2006**, *110*, 15666. c) B. J. Wiley, Y. Xiong, Z.-Y. Li, Y. Yin, Y. Xia, *Nano Lett.* **2006**, *6*, 765. d) B. Wiley, Y. Sun, Y. Xia, *Acc. Chem. Res.* **2007**, *40*, 1067.
- 15 a) Y. Gao, P. Jiang, D. F. Liu, H. J. Yuan, X. Q. Yan, Z. P. Zhou, J. X. Wang, L. Song, L. F. Liu, W. Y. Zhou, G. Wang, C. Y. Wang, S. S. Xie, *Chem. Phys. Lett.* **2003**, *380*, 146. b) Y. Gao, P. Jiang, D. F. Liu, H. J. Yuan, X. Q. Yan, Z. P. Zhou, J. X. Wang, L. Song, L. F. Liu, W. Y. Zhou, G. Wang, C. Y. Wang, S. S. Xie, *J. Phys. Chem. B* **2004**, *108*, 12877. c) Y. Gao, P. Jiang, L. Song, L. Liu, X. Yan, Z. Zhou, D. Liu, J. Wang, H. Yuan, Z. Zhang, X. Zhao, X. Dou, W. Zhou, G. Wang, S. Xie, *J. Phys. D: Appl. Phys.* **2005**, *38*, 1061. d) Y. Gao, L. Song, P. Jiang, L. F. Liu, X. Q. Yan, Z. P. Zhou, D. F. Liu, J. X. Wang, H. J. Yuan, Z. X. Zhang, X. W. Zhao, X. Y. Dou, W. Y. Zhou, G. Wang, S. S. Xie, H. Y. Chen, J. Q. Li, *J. Cryst. Growth* **2005**, 276, 606. e) Y. Gao, P. Jiang, L. Song, J. X. Wang, L. F. Liu, D. F. Liu, Y. J. Xiang, Z. X. Zhang, X. W. Zhao, X. Y. Dou, S. D. Luo, W. Y. Zhou, S. S. Xie, *J. Cryst. Growth* **2006**, 289, 376.
- 16 a) M. Tsuji, N. Miyamae, K. Matsumoto, S. Hikino, T. Tsuji, *Chem. Lett.* **2005**, *34*, 1518. b) M. Tsuji, N. Miyamae, S. Lim, K. Kimura, X. Zhang, S. Hikino, M. Nishio, *Cryst. Growth Des.* **2006**, *6*, 1801. c) M. Tsuji, M. Nishio, P. Jiang, N. Miyamae, S. Lim, K. Matsumoto, D. Ueyama, X. Tang, *Colloids Surf., A*, in press.
- 17 L. Vitos, A. V. Ruban, H. L. Skriver, J. Kollár, *Surf. Sci.* **1998**, *411*, 186.
- 18 a) M. Suzuki, M. Tanaka, M. Sato, Abstract of 6th International Symposium on Microwave Effects and the Applications, **2006**, pp. 93–94. b) M. Tanaka, M. Sato, *J. Chem. Phys.* **2007**, *126*, 034509.